Error Performance of Digital Modulation Schemes with MRC Diversity Reception over η-μ Fading Channels

Kostas Peppas, *Member, IEEE*, Fotis Lazarakis, Antonis Alexandridis, and Kostas Dangakis

***Abstract*—This paper provides exact-form expressions for the average symbol error probability (ASEP) of various digital modulation schemes with maximal ratio combining (MRC) diversity over L independent, not necessarily identically distributed (n.i.d.) η-μ fading channels. The derived expressions are given in terms of the Lauricella and Appell hypergeometric functions and include several others available in the literature such as those for Nakagami-m and Hoyt. General asymptotic ASEP expressions are also derived for all the considered modulation schemes which provide useful insights regarding the factors affecting the performance of the considered system.**

***Index Terms*—Digital modulation schemes, η-μ fading, average symbol error probability, maximal ratio combining diversity.**

I. Introduction

THE propagation of energy in a mobile radio environment is characterized by various effects including multipath fading and shadowing. A great number of distributions exist that well describe the statistics of the mobile radio signal. Among those which describe the short term signal variation, Rayleigh, Rice, Nakagami-m, Weibull and Hoyt are the well known distributions. However, in some specific situations, none of the above distributions seem to adequately fit experimental data, though one or another may yield a moderate fitting. Some researches even question the use of the Nakagami-m distribution because its tail does not seem to yield a good fitting to experimental data [1].

A relatively new model for fading channels is the so-called η-μ fading distribution [2]. The η-μ fading model is quite general as it includes the Hoyt and the Nakagami-m distributions as special cases. Moreover, it has been shown that it can accurately approximate the sum of independent non-identical Hoyt envelopes having arbitrary mean powers and arbitrary fading degrees [3].

In the context of performance evaluation of digital communications over fading channels this distribution has been used only recently. Representative past works can be found in [4], [5] and [6]. In [4], the average channel capacity of single branch receivers operating over η-μ channels was derived. In [5], expressions for the moment generating function (MGF) of the above mentioned channel were provided. Based on these results, the ASEP of coherent binary phase shift keying (BPSK) receivers operating over η-μ fading channels was obtained. Furthermore, in [6], using an approximate yet highly accurate expression for the sum of identical η-μ random variables, infinite series representations for the Outage Probability and ASEP of coherent and non coherent digital modulations for MRC and Equal Gain Combining (EGC) receivers are presented. The derived infinite series are given in terms of Meijer-G functions [7, Eq. (9.301)] and the ASEP results are valid for all average output signal-to-noise ratio (SNR) values for the case of binary modulation whereas for M-ary constellations are valid for high values of the average output SNR.

In this paper we derive novel closed-form expressions for the ASEP of M-ary phase shift keying (M-PSK), M-ary differential phase shift keying (M-DPSK) and general order rectangular quadrature amplitude modulation (QAM) using MRC diversity in n.i.d. η-μ fading channels. It is noted that MRC diversity provides the highest average output SNR that a diversity scheme can attain through fading channels [8]. The derived ASEP expressions are given in terms of Lauricella and Appell hypergeometric functions which can be easily evaluated numerically using their integral or converging series representation [9]. It is shown that our newly derived expressions incorporate as special cases several others available in the literature, namely those for Nakagami-m and Hoyt fading. Furthermore, in order to offer insights as to what parameters determine the performance of the considered modulation schemes under the presence of η-μ fading, a thorough asymptotic performance analysis at high SNR is performed.

The paper is structured as follows: In Section II, the considered channel model is described in detail. In Section III, closed form expressions for the ASEP of the considered modulation schemes are derived and their asymptotic behavior is investigated. In Section IV, numerical and computer simulation results are presented while the paper concludes with a summary given in Section V.

II. Channel Model

The η-μ fading model comprises both Hoyt ($\mu = 0.5$) and Nakagami-m ($\eta \to 0, \eta \to \infty, \eta \to \pm 1$) distributions. The corresponding probability density function (PDF) is expressed in two formats. In Format 1, the in-phase and quadrature components of the fading signal within each cluster are assumed to be independent from each other and to have different powers, with the parameter $0 < \eta < \infty$ given by the ratio between them. In Format 2, $-1 < \eta < 1$ denotes the correlation between the powers of the in-phase and quadrature scattered waves in each multi-path cluster. In both formats, the parameter $\mu > 0$ denotes the number of multi-path clusters. Assuming that signals are transmitted over

Manuscript received December 23, 2008; revised May 4, 2009; accepted July 14, 2009. The associate editor coordinating the review of this letter and approving it for publication was Dr. A. G. i Fabregas.

The authors are with Institute of Informatics and Telecommunications, National Centre for Scientific Research "Demokritos," 15310, Athens, Greece (e-mail: {kpeppas, flaz, aalex, kdang}@iit.demokritos.gr).

Digital Object Identifier 10.1109/TWC.2009.081687

L independently distributed η-μ branches with MRC diversity reception, the instantaneous SNR of the combiner output is given by $\gamma = \sum_{i=1}^{L} \gamma_i$ where γ_i is the instantaneous SNR of the i-th branch. The PDF of γ_i can be expressed as [4, Eq.(3)]:

$$f_{\gamma_i}(\gamma_i) = \frac{2\sqrt{\pi}\mu_i^{\mu_i+\frac{1}{2}} h_i^{\mu_i}}{\Gamma(\mu_i) H_i^{\mu_i-\frac{1}{2}}} \frac{\gamma_i^{\mu_i-\frac{1}{2}}}{\overline{\gamma}_i^{\mu_i+\frac{1}{2}}} \exp\left(-\frac{2\mu_i\gamma_i h_i}{\overline{\gamma}_i}\right) \times I_{\mu_i-\frac{1}{2}}\left(\frac{2\mu_i H_i \gamma_i}{\overline{\gamma}_i}\right) \tag{1}$$

where $\Gamma[\cdot]$ is the Gamma function [7, Eq. 8.310], $I_\nu[\cdot]$ is the modified Bessel function of the first kind and arbitrary order ν [7, Eq.(8.406.1)], $\overline{\gamma}_i = \mathbb{E}\langle\gamma_i\rangle$ is the average SNR with $\mathbb{E}\langle\cdot\rangle$ denoting expectation. In Format 1, $h_i = (2+\eta_i^{-1}+\eta_i)/4$ and $H_i = (\eta_i^{-1} - \eta_i)/4$ whereas in Format 2, $h_i = 1/(1-\eta_i^2)$ and $H_i = \eta_i/(1-\eta_i^2)$. The MGF of γ, defined as $\mathcal{M}_\gamma(s) = \mathbb{E}\langle\exp(-s\gamma)\rangle$, with the help of [5, Eq. (6)] can be expressed as :

$$\begin{aligned}\mathcal{M}_\gamma(s) &= \prod_{i=1}^{L} \int_0^\infty \exp(-s\gamma_i) f_{\gamma_i}(\gamma_i) d\gamma_i \\ &= \prod_{i=1}^{L} (1+A_i s)^{-\mu_i} (1+B_i s)^{-\mu_i}\end{aligned} \tag{2}$$

where $A_i = \frac{\overline{\gamma}_i}{2\mu_i(h_i - H_i)}$ and $B_i = \frac{\overline{\gamma}_i}{2\mu_i(h_i+H_i)}$, $i = 1 \cdots L$. It is also noted that for independent and identically distributed (i.i.d.) η-μ channels, the PDF of γ is an η-μ distribution with parameters η, $L\mu$ and $L\overline{\gamma}$ [6].

III. Expressions for the ASEP

A. M-ary PSK

The ASEP of M-ary PSK signals is given by [8, Eq. (5.78)]

$$P_s(e) = \mathcal{I}_1 + \mathcal{I}_2 \tag{3}$$

where

$$\begin{aligned}\mathcal{I}_1 &= \frac{1}{\pi} \int_{\pi/2}^{\pi-\pi/M} \mathcal{M}_\gamma\left(\frac{g_{PSK}}{\sin^2\theta}\right) d\theta, \\ \mathcal{I}_2 &= \frac{1}{\pi} \int_0^{\pi/2} \mathcal{M}_\gamma\left(\frac{g_{PSK}}{\sin^2\theta}\right) d\theta\end{aligned} \tag{4}$$

and $g_{PSK} = \sin^2(\pi/M)$. For the integral $\mathcal{I}_1$ by performing the change of variable $x = \cos^2\theta / \cos^2(\pi/M)$ and after some necessary manipulations, one obtains:

$$\begin{aligned}\mathcal{I}_1 &= \frac{\cos\left(\frac{\pi}{M}\right)}{2\pi} \int_0^1 x^{-\frac{1}{2}} \left(1 - x\cos^2\frac{\pi}{M}\right)^{-\frac{1}{2}} \\ &\times \prod_{i=1}^{L} \left(1 + \frac{A_i g_{PSK}}{1 - x\cos^2\frac{\pi}{M}}\right)^{-\mu_i} \\ &\times \prod_{i=1}^{L} \left(1 + \frac{B_i g_{PSK}}{1 - x\cos^2\frac{\pi}{M}}\right)^{-\mu_i} dx \\ &= \frac{1}{2\pi}\cos\left(\frac{\pi}{M}\right) \mathcal{M}_\gamma(g_{PSK}) \int_0^1 x^{-1/2} \\ &\left(1 - x\cos^2\frac{\pi}{M}\right)^{2\sum_{i=1}^{L}\mu_i - 1/2} \prod_{i=1}^{L} \left(1 - \frac{\cos^2\frac{\pi}{M}}{1+A_i g_{PSK}} x\right)^{-\mu_i} \\ &\times \prod_{i=1}^{L} \left(1 - \frac{\cos^2\frac{\pi}{M}}{1+B_i g_{PSK}} x\right)^{-\mu_i} dx \\ &= \frac{1}{\pi}\cos\left(\frac{\pi}{M}\right) \mathcal{M}_\gamma(g_{PSK}) F_D^{(2L+1)}\left(\frac{1}{2}, \frac{1}{2} - 2\sum_{i=1}^{L}\mu_i,\right. \\ &\mu_1, \cdots \mu_L, \mu_1, \cdots \mu_L; \frac{3}{2}; \cos^2\frac{\pi}{M}, \frac{\cos^2\frac{\pi}{M}}{1+A_1 g_{PSK}}, \cdots, \\ &\left.\frac{\cos^2\frac{\pi}{M}}{1+A_L g_{PSK}}, \frac{\cos^2\frac{\pi}{M}}{1+B_1 g_{PSK}} \cdots \frac{\cos^2\frac{\pi}{M}}{1+B_L g_{PSK}}\right)\end{aligned} \tag{5}$$

where $F_D^{(n)}(v, k_1, \cdots, k_n; c; z_1, \cdots, z_n)$ is the Lauricella multiple hypergeometric function of n variables defined as [10, Eq. (7.2.4.57)], [10, Eq. (7.2.4.15)]:

$$\begin{aligned}&F_D^{(n)}(v, k_1, \cdots, k_n; c; z_1, \cdots, z_n) = \\ &\frac{\Gamma(c)}{\Gamma(c-v)\Gamma(v)} \int_0^1 x^{v-1}(1-x)^{c-v-1} \prod_{i=1}^{n} (1-z_i x)^{-k_i} dx \\ &= \sum_{l_1, l_2, \cdots, l_n = 0}^{\infty} \frac{(v)_{l_T}}{(c)_{l_T}} \prod_{i=1}^{n} \frac{(k_i)_{l_i}}{\Gamma(i+1)} z_i^{l_i}, \ |z_i| < 1\end{aligned} \tag{6}$$

where $l_T = \sum_{i=1}^{n} l_i$, $(\alpha)_\beta = \Gamma(\alpha+\beta)/\Gamma(\alpha)$ is the Pochhammer symbol. The integral in (6) exists for $\Re\{c - v\} > 0$ and $\Re\{v\} > 0$ where $\Re\{\cdot\}$ denotes the real part. If $n = 2$, this function reduces to the Appell hypergeometric function F_1 [10, Eq. (7.2.1.41)] whereas if $n = 1$, it reduces to the Gauss hypergeometric function ${}_2F_1$. It is seen from (5) that the conditions for series convergence and integral existence of $F_D^{(2L+1)}$ are satisfied.

For the integral $\mathcal{I}_2$ by performing the change of variable $x = \cos^2\theta$ and after some manipulations we obtain:

$$\begin{aligned}\mathcal{I}_2 &= \frac{\mathcal{M}_\gamma(g_{PSK})}{2\pi} \int_0^1 x^{-\frac{1}{2}} (1-x)^{2\sum_{i=1}^{L}\mu_i - \frac{1}{2}} \\ &\times \prod_{i=1}^{L} \left(1 - \frac{1}{1+A_i g_{PSK}} x\right)^{-\mu_i} \\ &\times \prod_{i=1}^{L} \left(1 - \frac{1}{1+B_i g_{PSK}} x\right)^{-\mu_i} dx \\ &= \frac{\Gamma\left(2\sum_{i=1}^{L}\mu_i + 1/2\right)}{2\sqrt{\pi}\Gamma(2\sum_{i=1}^{L}\mu_i + 1)} \mathcal{M}_\gamma(g_{PSK}) F_D^{(2L)}\left(\frac{1}{2}, \mu_1, \cdots \mu_L,\right. \\ &\mu_1, \cdots \mu_L; 2\sum_{i=1}^{L}\mu_i + 1; \frac{1}{1+A_1 g_{PSK}}, \cdots, \frac{1}{1+A_L g_{PSK}}, \\ &\left.\frac{1}{1+B_1 g_{PSK}}, \cdots, \frac{1}{1+B_L g_{PSK}}\right)\end{aligned} \tag{7}$$

For the case of BPSK ($M = 2, g_{PSK} = 1$), it can be observed that $\mathcal{I}_1 = 0$ and therefore the expression for the ASEP is reduced to the following compact form:

$$P_s(e) = \frac{\Gamma\left(2\sum_{i=1}^{L}\mu_i + 1/2\right)}{2\sqrt{\pi}\Gamma(2\sum_{i=1}^{L}\mu_i + 1)}\mathcal{M}_\gamma(1)F_D^{(2L)}\left(\frac{1}{2}, \mu_1, \cdots \mu_L, \mu_1, \cdots \mu_L; 2\sum_{i=1}^{L}\mu_i + 1; \frac{1}{1+A_1}\cdots, \frac{1}{1+A_L}, \frac{1}{1+B_1}, \cdots, \frac{1}{1+B_L}\right) \tag{8}$$

For the i.i.d. case, where $h_i = h$, $H_i = H$, $\mu_i = \mu$, $A_i = A$ and $B_i = B$, using the integral representation of $F_D^{(2L+1)}$ and $F_D^{(2L)}$, the following simplified forms are obtained:

$$\mathcal{I}_{1_{iid}} = \frac{1}{\pi}\cos\left(\frac{\pi}{M}\right)\mathcal{M}_\gamma(g_{PSK})F_D^{(3)}\left(\frac{1}{2}, \frac{1}{2} - 2L\mu, L\mu, L\mu; \frac{3}{2}; \cos^2\frac{\pi}{M}, \frac{\cos^2\frac{\pi}{M}}{1+Ag_{PSK}}, \frac{\cos^2\frac{\pi}{M}}{1+Bg_{PSK}}\right) \tag{9}$$

$$\mathcal{I}_{2_{iid}} = \frac{\Gamma(2L\mu + 1/2)}{2\sqrt{\pi}\Gamma(2L\mu+1)}\mathcal{M}_\gamma(g_{PSK})F_1\left(\frac{1}{2}, L\mu, L\mu; 2L\mu + 1; \frac{1}{1+Ag_{PSK}}, \frac{1}{1+Bg_{PSK}}\right) \tag{10}$$

For the special case of Hoyt fading channels ($\mu = 0.5$) and no diversity ($L = 1$), the expression for the ASEP of M-ary PSK is reduced to a previously known result [11, Eq. (18)]. Finally, for Nakagami-m fading channels and i.i.d. branches, using (10) and [10, Eq. (7.2.4.60)], a previously known result may be obtained [12, Eq. (6)].

In [13], the authors developed a simple and general method to quantify the asymptotic performance of wireless transmission in fading channels at high SNR values. In this work, it was shown that the asymptotic performance depends on the behavior of the PDF of the instantaneous channel power gain denoted by β, $p(\beta)$. Moreover, it was shown that if the MGF of $p(\beta)$ can be expressed for $s \to \infty$ as $|\mathcal{M}_\beta(s)| = C|s|^{-d} + o(|s|^{-d})$, a diversity gain equal to d may be obtained. It is noted that we write $f(x) = o[g(x)]$ as $x \to x_0$ if $\lim_{x\to x_0}\frac{f(x)}{g(x)} = 0$. We observe that (2) can be expressed as:

$$\begin{aligned}\mathcal{M}_\gamma(s) &= \prod_{i=1}^{L}\left[s^{-2}A_iB_i\left(1+\frac{1}{A_is}\right)\left(1+\frac{1}{B_is}\right)\right]^{-\mu_i} \\ &= Cs^{-d} + o(s^{-d})\end{aligned} \tag{11}$$

for $s \to \infty$, where $C = \prod_{i=1}^{L}(A_iB_i)^{-\mu_i} = \prod_{i=1}^{L}h_i^{\mu_i}\left(\frac{\overline{\gamma}_i}{2\mu_i}\right)^{-2\mu_i}$ and $d = 2\sum_{i=1}^{L}\mu_i$. This interesting result shows that the diversity gain of the considered system depends on the number of the receive antennas L as well as on the parameters μ_i. For the special case of i.i.d. branches, it is obvious that a diversity gain equal to $2\mu L$ may be obtained.

At high SNR, using the previously derived asymptotic expression for the MGF, $\mathcal{I}_1$ can be computed as:

$$\begin{aligned}\mathcal{I}_{1_{asym}} &= \frac{C\cos\frac{\pi}{M}}{2g_{PSK}^d\pi}\int_0^1 x^{-1/2}\left(1 - x\cos^2\frac{\pi}{M}\right)^{-1/2+d}dx \\ &= \frac{C\cos\frac{\pi}{M}}{\pi g_{PSK}^d}{}_2F_1\left(\frac{1}{2}-d, \frac{1}{2}; \frac{3}{2}; \cos^2\frac{\pi}{M}\right)\end{aligned} \tag{12}$$

Also, a simplified asymptotic expression of $\mathcal{I}_2$ may be obtained as:

$$\mathcal{I}_{2_{asym}} = \frac{C}{g_{PSK}^d\pi}\int_0^{\pi/2}\sin^{2d}\theta d\theta = \frac{C\Gamma(d+1/2)}{2\sqrt{\pi}\Gamma(d+1)g_{PSK}^d} \tag{13}$$

B. M-ary DPSK

The ASEP of M-ary DPSK signals is given by [8, Eq. (8.200)]

$$P_s(e) = \frac{2}{\pi}\int_0^{\pi/2-\pi/2M}\mathcal{M}_\gamma\left(\zeta\sin^2\frac{\pi}{M}\right)d\theta \tag{14}$$

where $\zeta = \left(1 + \cos\frac{\pi}{M} - 2\cos\frac{\pi}{M}\sin^2\theta\right)^{-1}$. Applying the transformation $x = \sin^2\theta/\cos^2(\pi/2M)$ and after some algebraic manipulations the ASEP of M-ary DPSK can be expressed as:

$$\begin{aligned}P_s(e) &= \frac{\cos\left(\frac{\pi}{2M}\right)}{\pi}\mathcal{M}_\gamma(f(M))\int_0^1 x^{-\frac{1}{2}}\left(1 - x\cos^2\frac{\pi}{2M}\right)^{-\frac{1}{2}} \\ &\times\left(1 - x\cos\frac{\pi}{M}\right)^{2\sum_{i=1}^{L}\mu_i}\prod_{i=1}^{L}\left(1 - \frac{\cos\frac{\pi}{M}}{1+A_if(M)}x\right)^{-\mu_i} \\ &\times\prod_{i=1}^{L}\left(1 - \frac{\cos\frac{\pi}{M}}{1+B_if(M)}x\right)^{-\mu_i}dx \\ &= \frac{2}{\pi}\cos\left(\frac{\pi}{2M}\right)\mathcal{M}_\gamma(f(M))F_D^{(2L+2)}\left(\frac{1}{2}, \frac{1}{2}, -2\sum_{i=1}^{L}\mu_i, \mu_1, \mu_1, \cdots, \mu_L, \mu_L; \frac{3}{2}; \cos^2\frac{\pi}{2M}, \cos\frac{\pi}{M}, \frac{\cos\frac{\pi}{M}}{1+A_1f(M)}, \frac{\cos\frac{\pi}{M}}{1+B_1f(M)}, \cdots, \frac{\cos\frac{\pi}{M}}{1+A_Lf(M)}, \frac{\cos\frac{\pi}{M}}{1+B_Lf(M)}\right)\end{aligned} \tag{15}$$

where $f(M) = \frac{\sin^2(\pi/M)}{2\cos^2(\pi/2M)}$.

For binary DPSK signals ($M = 2$), using $F_D^{(N)}(v, k_1, k_2, \cdots, k_N; c; z, 0, \cdots, 0) = {}_2F_1(v, k_1; c; z)$ and ${}_2F_1\left(\frac{1}{2}, \frac{1}{2}; \frac{3}{2}; z\right) = \arcsin(\sqrt{z})/\sqrt{z}$ [10, Eq. (7.3.2.76)], the derived result is reduced to the well known expression for the error probability of binary DPSK signals over generalized fading channels, i.e. $P_{M=2}(e) = \frac{1}{2}\mathcal{M}_\gamma(1)$.

For the i.i.d. case, using the integral representation of the Lauricella function, a simplified expression of $P_s(e)$ may be obtained as:

$$P_s(e) = \frac{2\cos\left(\frac{\pi}{2M}\right)\mathcal{M}_\gamma(f(M))}{\pi}F_D^{(4)}\left(\frac{1}{2}, \frac{1}{2}, -2L\mu, L\mu, L\mu; \frac{3}{2}; \cos^2\frac{\pi}{2M}, \cos\frac{\pi}{M}, \frac{\cos\frac{\pi}{M}}{1+Af(M)}, \frac{\cos\frac{\pi}{M}}{1+Bf(M)}\right) \tag{16}$$

For high SNR values, by substituting (11) to (14) and using the same methodology for the evaluation of the corresponding integral, the following asymptotic expression of $P_s(e)$ may be obtained as:

$$\begin{aligned} P_s(e) &= \frac{C[f(M)]^{-d}}{\pi}\cos\left(\frac{\pi}{2M}\right)\int_0^1 x^{-1/2}\left(1-x\cos\frac{\pi}{M}\right)^d \\ &\quad\times\left(1-x\cos^2\frac{\pi}{2M}\right)^{-1/2}dx \\ &= \frac{2C[f(M)]^{-d}}{\pi}\cos\left(\frac{\pi}{2M}\right)F_1\left(\frac{1}{2},\frac{1}{2},-d;\frac{3}{2};\cos^2\frac{\pi}{2M},\right. \\ &\quad\left.\cos\frac{\pi}{M}\right) \end{aligned} \tag{17}$$

C. General Order Rectangular QAM

We consider a general order rectangular QAM signal which may be viewed as two separate Pulse Amplitude Modulation (PAM) signals impressed on phase-quadrature carriers. Let also M_I and M_Q be the dimensions of the in-phase and the quadrature signal respectively and $r = d_Q/d_I$ the quadrature-to-in-phase decision distance ratio, with d_I and d_Q being the in-phase and the quadrature decision distance respectively. For general order rectangular QAM, the ASEP is given by [14, Eq. (4)]

$$P_s(e) = 2p\mathcal{J}(a) + 2q\mathcal{J}(b) - 4pq[\mathcal{K}(a,b)+\mathcal{K}(b,a)] \tag{18}$$

where

$$\begin{aligned} \mathcal{J}(t) &= \frac{1}{\pi}\int_0^{\pi/2}\mathcal{M}_\gamma\left(\frac{t^2}{2\sin^2\theta}\right)d\theta, \\ \mathcal{K}(u,v) &= \frac{1}{2\pi}\int_0^{\pi/2-\arctan(v/u)}\mathcal{M}_\gamma\left(\frac{u^2}{2\sin^2\theta}\right)d\theta \end{aligned} \tag{19}$$

and $p = 1-1/M_I$, $q = 1-1/M_Q$, $a = \sqrt{\frac{6}{(M_I^2-1)+r^2(M_Q^2-1)}}$, $b = \sqrt{\frac{6r^2}{(M_I^2-1)+r^2(M_Q^2-1)}}$. Using the result in (7), the integral $\mathcal{J}(t)$ can be easily evaluated in terms of the Lauricella functions as:

$$\begin{aligned} \mathcal{J}(t) &= \frac{\Gamma\left(2\sum_{i=1}^L\mu_i+1/2\right)}{2\sqrt{\pi}\Gamma(2\sum_{i=1}^L\mu_i+1)}\mathcal{M}_\gamma(t^2/2)F_D^{(2L)}\left(\frac{1}{2},\right. \\ &\mu_1,\cdots\mu_L,\mu_1,\cdots\mu_L;2\sum_{i=1}^L\mu_i+1;\frac{2}{2+A_1t^2},\cdots,\frac{2}{2+A_Lt^2}, \\ &\left.\frac{2}{2+B_1t^2},\cdots,\frac{2}{2+B_Lt^2}\right) \end{aligned} \tag{20}$$

To evaluate $\mathcal{K}(u,v)$ in (19), applying the transformation $x = 1-(v^2/u^2)\tan^2\theta$ and after performing some algebraic and trigonometric manipulations, we obtain:

$$\begin{aligned} \mathcal{K}(u,v) &= \frac{uv\mathcal{M}_\gamma(\frac{u^2+v^2}{2})}{4\pi(u^2+v^2)}\int_0^1(1-x)^{2\sum_{i=1}^L\mu_1-\frac{1}{2}} \\ &\times\left(1-\frac{u^2}{u^2+v^2}x\right)^{-1}\prod_{i=1}^L\left(1-x\frac{2+A_iu^2}{2+A_iu^2+A_iv^2}\right)^{-\mu_i} \\ &\times\prod_{i=1}^L\left(1-x\frac{2+B_iu^2}{2+B_iu^2+B_iv^2}\right)^{-\mu_i}dx \\ &= \frac{uv\mathcal{M}_\gamma(\frac{u^2+v^2}{2})}{2\pi(u^2+v^2)\left(4\sum_{i=1}^L\mu_i+1\right)}F_D^{(2L+1)}\left(1,1,\mu_1,\cdots,\mu_L,\right. \\ &\mu_1,\cdots,\mu_L;2\sum_{i=1}^L\mu_i+\frac{3}{2};\frac{u^2}{u^2+v^2},\frac{2+A_1u^2}{2+A_1u^2+A_1v^2},\cdots, \\ &\frac{2+A_Lu^2}{2+A_Lu^2+A_Lv^2},\frac{2+B_1u^2}{2+B_1u^2+B_1v^2},\cdots, \\ &\left.\frac{2+B_Lu^2}{2+B_Lu^2+B_Lv^2}\right) \end{aligned} \tag{21}$$

For i.i.d. branches (20) reduces to:

$$\begin{aligned} \mathcal{J}_{iid}(t) &= \frac{\Gamma(2L\mu+1/2)}{2\sqrt{\pi}\Gamma(2L\mu+1)}\mathcal{M}_\gamma(t^2/2) \\ &F_1\left(\frac{1}{2},L\mu,L\mu;2L\mu+1;\frac{2}{2+At^2},\frac{2}{2+Bt^2}\right) \end{aligned} \tag{22}$$

whereas (21) is reduced to:

$$\begin{aligned} \mathcal{K}_{iid}(u,v) &= \frac{uv\mathcal{M}_\gamma(\frac{u^2+v^2}{2})}{2\pi(u^2+v^2)(4L\mu+1)}F_D^{(3)}\left(1,1,L\mu,L\mu;\right. \\ &\left.2L\mu+\frac{3}{2};\frac{u^2}{u^2+v^2},\frac{2+Au^2}{2+Au^2+Av^2},\frac{2+Bu^2}{2+Bu^2+Bv^2}\right) \end{aligned} \tag{23}$$

For the special case of Nakagami-m channels, using [10, Eq. (7.2.4.60)], (22) is reduced to a previously known result [14, Eq. 11]. Moreover, using the infinite series representation of the Lauricella function (6), [10, Eq. (7.2.4.60)] and after some necessary manipulations, (23) is reduced to a previously known result [14, Eq. 15].

For high SNR values, the following asymptotic form for $\mathcal{J}(t)$ may be obtained:

$$\mathcal{J}_{asym}(t) = \frac{2^dC}{t^{2d}\pi}\int_0^{\pi/2}\sin^{2d}\theta d\theta = \frac{2^{d-1}C\Gamma(d+1/2)}{\sqrt{\pi}\Gamma(d+1)t^{2d}} \tag{24}$$

Moreover, using the integral representation of the ${}_2F_1$ function, a simplified asymptotic expression for $\mathcal{K}(u,v)$ may be obtained, as:

$$\begin{aligned} \mathcal{K}_{asym}(u,v) &= \frac{2^{d-2}Cuv}{\pi(u^2+v^2)^{d+1}}\int_0^1(1-x)^{d-1/2} \\ &\times\left(1-\frac{u^2}{u^2+v^2}x\right)^{-d-1}dx \\ &= \frac{2^{d-1}Cuv}{\pi(u^2+v^2)^{d+1}(2d+1)}{}_2F_1\left(1,d+1;d+\frac{3}{2};\frac{u^2}{u^2+v^2}\right) \end{aligned} \tag{25}$$

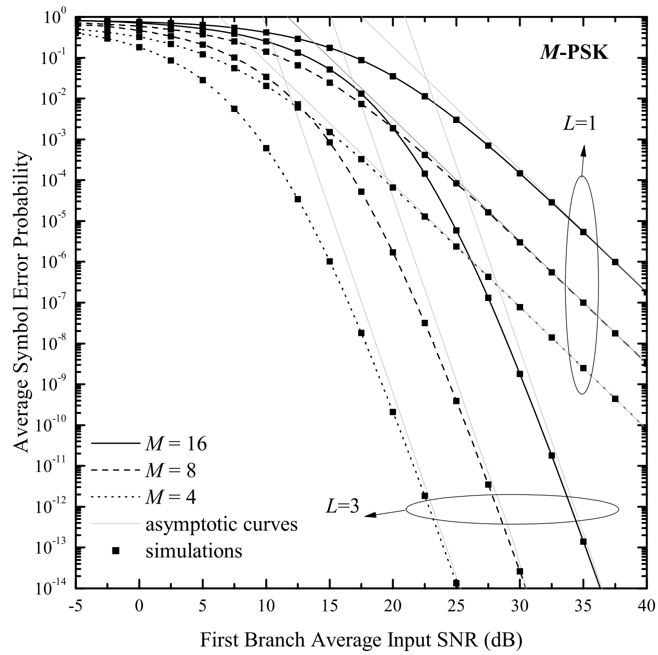

Fig. 1. Average Symbol Error Probability of M-PSK receivers with MRC diversity ($L = 1, 3$) operating over n.i.d. η-μ fading channels, for different values of M, as a function of the First Branch Average Input SNR ($\eta = 2$, $\mu = 1.5$, $\delta = 0.5$)

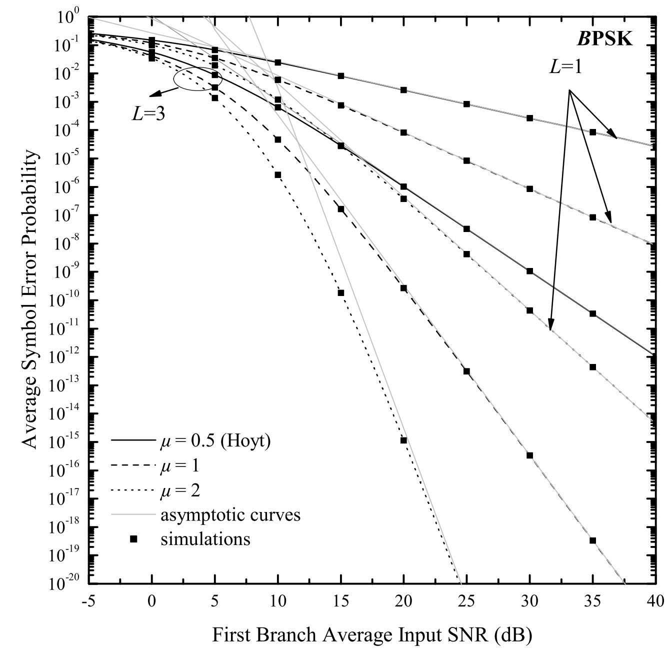

Fig. 2. Average Symbol Error Probability of BPSK receivers with MRC diversity ($L = 1, 3$) operating over n.i.d. η-μ fading channels, for $\eta = 2$ and for different values of μ, as a function of the First Branch Average Input SNR ($\delta = 0.5$)

IV. Numerical Results and Discussion

In this section, using the above formulations, numerical results concerning the error rate performance of M-PSK, M-DPSK and general order QAM systems, are presented, together with computer simulations. The Lauricella functions, were numerically evaluated using their integral representation. For n.i.d. branches, an exponential power decay profile is considered, that is the average input SNR of the l-th branch is given by $\overline{\gamma}_l = \overline{\gamma}_1 \exp[-\delta(l-1)]$ where δ is the decay factor. For all test cases, we assume $\delta = 0.5$.

In Fig. 1 the ASEP of M-PSK modulation is plotted as a function of the first branch average input SNR $\overline{\gamma}_1$, for the η-μ fading channel, Format 1 and for different values of M and L, with $\eta_\ell = \eta = 2$ and $\mu_\ell = \mu = 1.5$, $\ell = 1, 2, 3$. As expected, an increase in the number of diversity branches from $L = 1$ to $L = 3$ significantly enhances the system's error performance. In the same figure, the exact and the asymptotic ASEP results are also compared. As it is evident, the asymptotic results correctly predict the diversity gain, however for large M and L, the predicted asymptotic behavior of the ASEP curves shows up at relatively high SNR (e.g. for $M = 16$, $L = 3$ we need $\overline{\gamma}_1 > 30$dB). To further examine the effect of the μ fading parameter on the performance of the considered system, in Fig. 2 the ASEP for BPSK modulation is plotted as a function of $\overline{\gamma}_1$ for constant η equal to 2 and for various values of μ and L. As expected, by keeping η constant, an increase in μ and/or L results in an improvement of the system performance. For comparison purposes, for $L = 1, 2$ and 3, the ASEP of the BPSK modulation for the Hoyt fading channel ($\mu = 0.5$) has also been plotted versus the average input SNR per branch. It is obvious that the Hoyt channel results in the worst symbol error performance. The asymptotic performance of the BPSK ASEP expressions is also investigated and as it can be observed, for no diversity ($L = 1$) and small values of μ, the high SNR asymptotic expressions yield accurate results even for low to medium SNR values.

In Fig. 3 similar results for M-DPSK signal constellations are given with $\eta_\ell = \eta = 2$, $\mu_\ell = \mu = 1.5$ and $L = 1, 3$. As in the case of coherent modulation, the performance of the considered system significantly improves as the number of diversity branches increases. Also in Fig. 4 the effect of the η fading parameter on the performance of the considered system is illustrated specifically for BDPSK. In this test case, μ is kept constant and equal to 2. It is observed that by keeping μ constant, the ASEP decreases as η decreases and/or L increases. In both figures, asymptotic results are also included and as it can be observed, the asymptotic approximation predicts the diversity gain correctly and provides good approximation to the exact error performance in the high SNR region, especially when L is small.

In Figs. 5 and 6 the error performance of a 8×4 QAM system is illustrated for two test cases, namely $\eta = 2$ and $\mu = 1.5$ for i.i.d. and n.i.d. branches with $\delta = 0.5$. In both figures, the ASEP is plotted for different values of L and r and as it is obvious, the error performance significantly improves as L increases. Also, from both figures, it can be observed that the ASEP deteriorates substantially as r increases, for all values of μ. Moreover, in Fig. 6, asymptotic results have been included and as it is evident, the simplified asymptotic expressions yield accurate results at high SNR values, especially when L and/or r are small.

Finally, for all the considered modulation schemes, equivalent computer simulation results were included and an excellent match with the analytically obtained results is observed.

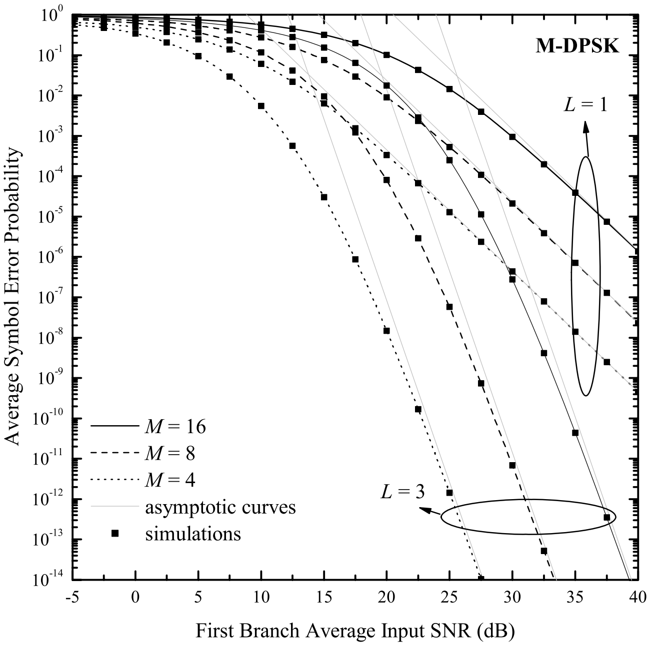

Fig. 3. Average Symbol Error Probability of M-DPSK receivers with MRC diversity $(L = 1, 3)$ operating over n.i.d. η-μ fading channels, for different values of M, as a function of the First Branch Average Input SNR ($\eta = 2$, $\mu = 1.5$, $\delta = 0.5$)

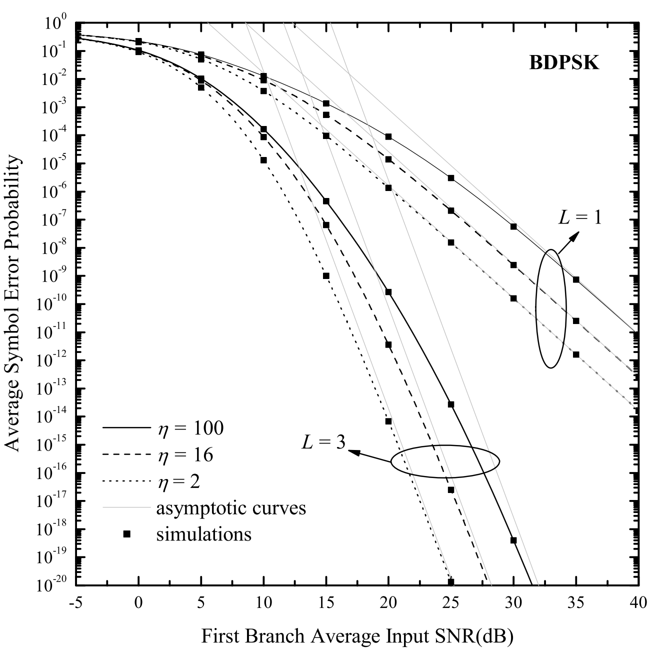

Fig. 4. Average Symbol Error Probability of BDPSK receivers with MRC diversity $(L = 1, 3)$ operating over n.i.d. η-μ fading channels, for $\mu = 2$ and for different values of η, as a function of the First Branch Average Input SNR ($\delta = 0.5$)

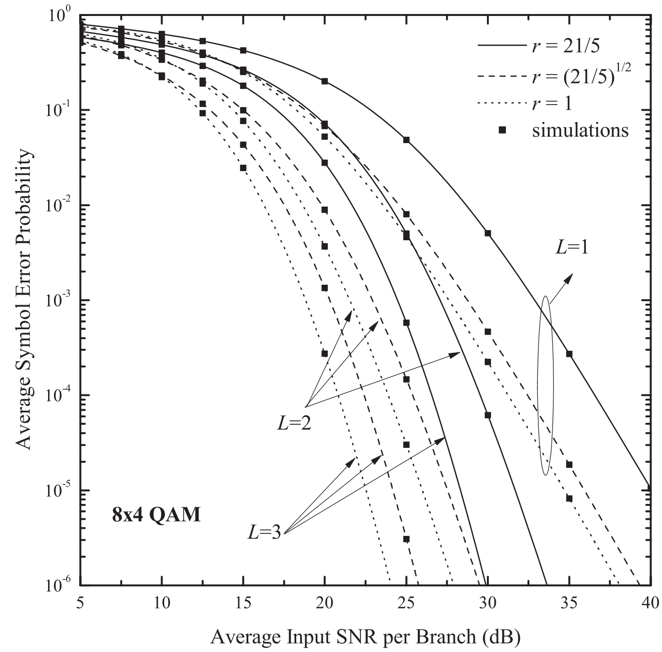

Fig. 5. Average Symbol Error Probability of 8×4 QAM receivers with MRC diversity $(L = 1, 2, 3)$ operating over i.i.d. η-μ fading channels, for different values of r, as a function of the Average Input SNR per Branch ($\eta = 2$, $\mu = 1.5$)

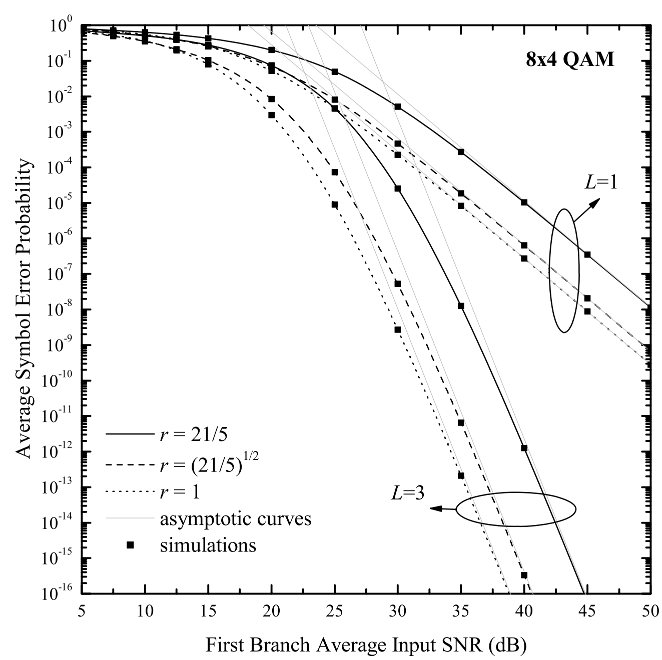

Fig. 6. Average Symbol Error Probability of 8×4 QAM receivers with MRC diversity $(L = 1, 3)$ operating over n.i.d. η-μ fading channels, for different values of r, as a function of the First Branch Average Input SNR ($\eta = 2$, $\mu = 1.5$, $\delta = 0.5$)

V. Conclusion

In this paper, we have derived novel closed-form expressions for the ASEP of M-PSK, M-DPSK and general order rectangular QAM receivers with MRC diversity operating over independent, not necessarily identically distributed η-μ fading channels. Our results were validated by reducing them to several special cases available in the literature, namely those for Nakagami-m and Hoyt fading channels as well as by means of computer simulations. High SNR asymptotic expressions for the ASEP of all the considered modulation schemes were derived which demonstrated that the achieved diversity gain depends on the number of the receive antennas as well as on the parameters μ in each branch of the receiver.

References

[1] S. Stein, "Fading channel issues in system engineering," *IEEE J. Select. Areas Commun.*, vol. 5, no. 2, pp. 68-69, Feb. 1987.

[2] M. D. Yacoub, "The κ-μ and the η-μ distribution," *IEEE Antennas Propag. Mag.*, vol. 49, no. 1, pp. 68-81, Feb. 2007.

[3] J. C. S. S. Filho, and M. D. Yacoub, "Highly accurate η-μ approximation to sum of m independent non-identical Hoyt variates," *IEEE Antennas Wireless Propag. Lett.*, vol. 4, pp. 436-438, 2005.

[4] D. B. da Costa and M. D. Yacoub, "Average channel capacity for generalized fading scenarios," *IEEE Commun. Lett.*, vol. 11, no. 12, pp. 949-951, Dec. 2007.

[5] N. Ermolova, "Moment generating functions of the generalized $\eta - \mu$ and $k - \mu$ distributions and their applications to performance evaluations of communication systems," *IEEE Commun. Lett.*, vol. 12, no. 7, pp. 502-504, July 2008.

[6] D. B. da Costa and M. D. Yacoub, "Accurate closed-form approximations to the sum of generalized random variables and applications," in *Proc. IEEE Wireless Communications and Networking Conference (WCNC)*, 2008, pp. 785-790.

[7] I. Gradshteyn and I. M. Ryzhik, *Tables of Integrals, Series, and Products*, 6th ed. New York: Academic Press, 2000.

[8] M. K. Simon and M. S. Alouini, *Digital Communication over Fading Channels*, 2nd ed. New York: Wiley, 2005.

[9] G. P. Efthymoglou, T. Piboongungon, and V. A. Aalo, "Error rates of M-ary signals with multichannel reception in Nakagami-m fading channels," *IEEE Commun. Lett.*, vol. 10, no. 2, pp. 100-102, Feb. 2006.

[10] A. P. Prudnikov, Y. A. Brychkov, and O. I. Marichev, *Integrals and Series, Volume 3: More Special Functions*, 1st ed. Gordon and Breach Science Publishers, 1986.

[11] R. M. Radaydeh, "Average error performance of m-ary modulation schemes in Nakagami-q (Hoyt) fading channels," *IEEE Commun. Lett.*, vol. 11, no. 3, pp. 255-257, Mar. 2007.

[12] A. Adinoyi and S. Al-Semari, "Expression for evaluating performance of BPSK with MRC in Nakagami fading," *IEE Electron. Lett.*, vol. 38, no. 23, pp. 1428-1429, Nov. 2002.

[13] Z. Wang and G. Yannakis, "A simple and general parametrization quantifying performance in fading channels," *IEEE Trans. Commun.*, vol. 51, no. 8, pp. 1389-1398, Aug. 2003.

[14] X. Lei, P. Fan, and L. Hao, "Exact symbol error probability of general order rectangular QAM with MRC diversity reception over Nakagami-m fading channels," *IEEE Commun. Lett.*, vol. 11, no. 12, pp. 958-960, Mar. 2007.